

# PlaNet-Pick: Effective Cloth Flattening Based on Latent Dynamic Planning

Halid Abdulrahim Kadi<sup>1,\*</sup> and Kasim Terzić<sup>1,†</sup>

March 3, 2023

## Abstract

Why do Recurrent State Space Models such as PlaNet fail at cloth manipulation tasks? Recent work has attributed this to the blurry reconstruction of the observation, which makes it difficult to plan directly in the latent space. This paper explores the reasons behind this by applying PlaNet in the pick-and-place cloth-flattening domain. We find that the sharp discontinuity of the transition function on the contour of the article makes it difficult to learn an accurate latent dynamic model. By adopting *KL balancing* and *latent overshooting* in the training loss and adjusting the planned picking position to the closest part of the cloth, we show that the updated PlaNet-Pick model can achieve state-of-the-art performance using latent MPC algorithms in simulation.

## 1 Introduction

Deep reinforcement learning methods based on Recurrent State Space Model (RSSM), such as PlaNet [13] and Dreamers [12, 14, 15] have achieved state-of-the-art asymptotic performance and data efficiency in both continuous control `dm_control` [34] and discrete-action Atari 2600 [2] benchmark environments. However, planning on RSSM-based models keeps failing a canonical task in cloth-shaping: cloth flattening [28, 39, 26, 27, 20], where one or more end-effectors operate on a piece of square fabric to unfold it on a surface (Figure 1).

Most successful data-driven methods, such as imitation learning [33, 35, 32] and reinforcement learning [24, 39, 37, 17, 28, 26, 19], for cloth-flattening focus on quasi-static pick-and-place (P&P) manipulation. Despite pick-and-throw and pick-and-blow primitives being operationally more effective than quasi-static P&P primitives [38, 10], P&P still important because it is based on safe and predictable actions.

Deep Planning Network (PlaNet) [13] is a model-based reinforcement learning algorithm that uses model-predictive control to plan on a latent dynamic model trained based on the RSSM (Section 3.1). However, PlaNet keeps failing on cloth flattening [28, 39, 26, 27]; it has been argued that this may be due to the blurry observation reconstruction of the latent dynamic model [18, 26]. We thoroughly investigate PlaNet’s performance on the cloth-flattening domain in simulation benchmark SoftGym [27] to understand the causes of poor performance on this task. We note five potential areas of improvement to the original PlaNet model:

- The fundamental reason that PlaNet fails at P&P cloth-flattening is that the original algorithm feeds out-of-bounds candidate actions into the latent dynamic model while planning. Therefore, we propose to clip the actions between its trained boundary before rolling out with the model and to update the normal distributions with these clipped actions.
- We also observe that the latent dynamic model of PlaNet cannot learn a good latent prior distribution due to the complex non-linear behaviour of CDO. Therefore, we adopt *KL balancing* [14] to improve both posterior and prior learning quality.
- Default one-step prior learning of PlaNet is susceptible to the horizon length of planning algorithms, so we also include *latent overshooting* [13] to improve the robustness of the latent planning.
- Latent dynamic models need a large amount of data to overcome the enormity and complexity of the cloth’s dynamic. Hence, we employ data augmentation techniques, such as rotation [24] and flipping, to upsample the sampled trajectories to improve the data efficiency and robustness of the model.

<sup>\*1</sup> School of Computer Science, University of St Andrews, Jack Cole Building, North Haugh, St Andrews, KY16 9SX United Kingdom

<sup>†\*</sup> Correspondence author, E-mail: ah390@st-andrews.ac.uk; Tel.: +44 1334 46 1630

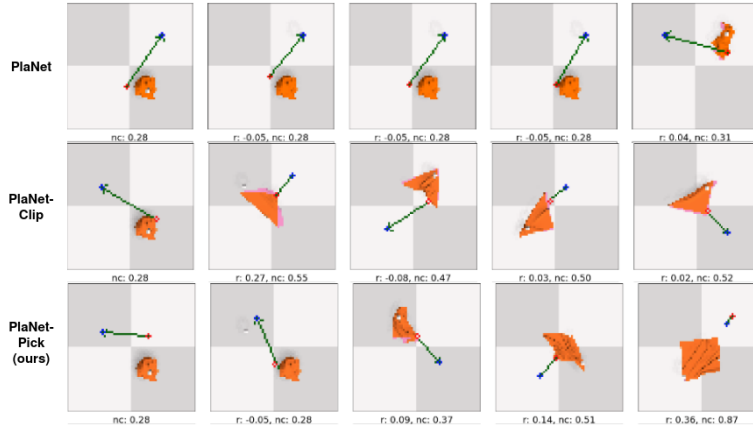


Figure 1: Execution Trajectories using MPC (100 iterations, 5000 candidates, pick readjustment) in SoftGym [27]. Red targets are the unadjusted pick positions from planning.

- Finally, to address the difficulty in accurately modelling the sharp discontinuity on the contour of the article, we apply a small readjustment technique on the picking action to improve operational efficiency.

We demonstrate that these five improvements lead to PlaNet achieving state-of-the-art (SOTA) performance on cloth flattening, showing that RSSM-based algorithms can play an important role in a wider range of application domains.

## 2 Related Work

Model-based reinforcement learning (MBRL) applications in P&P cloth-flattening are mainly Type I [29]: planning or trajectory optimisation algorithms, where the agent needs access to the dynamic model of the environment for generating imaginary rollouts. The dynamic model can be either a known dynamic or a learned dynamic. Planning algorithms used in cloth-flattening are mainly based on model-predictive control (MPC), which can be split into goal-conditioned MPC (GC-MPC) [16, 40] and reward-based MPC (R-MPC) systems [28, 26, 19].

Visual Foresight (VSF) [17] by Hoque et al. (based on Visual MPC [7]) and the Contrastive Forward Model (CFM) [40] by Yan et al. are the two example applications of GC-MPC to cloth flattening, where the cost function is calculated based on the difference between the current and goal states. R-MPC, on the other hand, selects elite trajectories based on reward prediction from the prior rollout trajectories. In contrast to GC-MPC, the application domain of R-MPC is limited by the reward prediction function given to the algorithm. Ma et al.’s (2021) latent graph dynamics for DefOrmable Object Manipulation (G-DOOM) is a latent R-MPC method which generates the prior rollout trajectories at the latent space. Lin et al. (2022)’s Visible Connectivity Dynamics (VCD) [26], on the other hand, is a Mesh R-MPC method that rollouts on the reconstructed mesh representation using a learned mesh dynamic [30]. Although Mesh R-MPC methods, such as VCD [26] and MEDOR [19], outperform GC-MPC and latent R-MPC methods, they are difficult to implement and harder to generalise across tasks compared to latent MPC.

Deep Planning Network (PlaNet) [13] is a latent R-MPC method that employs a learned latent dynamic based on a Recurrent State Space Model (RSSM). While it performs well on continuous control benchmark environments like the `dm_control` suite [34], numerous experiments have found it unsuitable for cloth flattening [40, 28, 27]. A possible reason is that the reconstructed observation from the visual model is fuzzy, which makes planning based on reconstructed vision hard due to the lack of precision around edges and corners of the article [26].

Dreamer [12, 14, 15] is a model-based actor-critic (AC) reinforcement learning algorithm that uses RSSM [13] for representation learning. It shows significant data efficiency and performance improvement compared to the PlaNet and AC baselines, and Dreamer V2 [14] is the first MBRL algorithm to achieve super-human performance with a single GPU in discrete-action Atari benchmarks. The architecture and objective of the latent dynamic model of Dreamer are directly inherited from PlaNet’s [13]. Dreamer V2 [14] leverages categorical latent state space representation and *KL balancing* to learn the latent dynamic model.

Stochastic Latent Actor-Critic (SLAC) [23] combines the Soft Actor-Critic’s (SAC) [11] maximum-entropy RL objective [42, 25] with latent dynamic representation learning to solve *Partially Observable Markov Decision*

*Processes* (POMDP) [21]. In contrast to RSSM-based algorithms such as PlaNet and Dreamer, it only learns stochastic latent representation. It exhibits stability, data efficiency and improved performance compared to SAC and PlaNet in several benchmarks [23] but has never been tested on CDO manipulation tasks. We evaluate the performance of SLAC’s latent dynamic model in this paper (Section 4.2).

### 3 Method

We wish to investigate the failure of PlaNet in cloth flattening to develop a model capable of handling this domain. A latent dynamic model for pick-and-place cloth flattening must accurately predict future states based on a sequence of future action trajectories to allow a planning algorithm to generate a trajectory of candidate actions that minimises a cost function. We can formulate the model learning problem as a partially-observable Markov decision process (POMDP).

*Problem Setting:* Our environment is built on SoftGym’s [27] cloth-flattening task with pick-and-place action extension, which comprises 4 parameters  $(x_{pick}, y_{pick}, x_{place}, y_{place})$  defined on continuous pixel space  $[-1, 1]$  for a single picker operation. We bound the action parameters in  $[-0.5, 0.5]$  to avoid the article’s out-of-view scenarios. The observations are RGB images collected from a top-down camera. The reward is adopted from Hoque et al. (2022) [17], where the relative coverage improvement between two consecutive states is the base of the reward function, and it penalises misgrasping (-0.05) steps and credits (+1) the high coverage states.

#### 3.1 Deep Planning Network (PlaNet)

RSSM [13] is defined under the POMDP setting with the following latent state dynamic: (1) recurrent dynamic model  $\mathbf{h}_t = f(\mathbf{h}_{t-1}, \mathbf{z}_{t-1}, \mathbf{a}_{t-1})$ , (2) representation model  $\hat{\mathbf{z}}_t \sim q(\hat{\mathbf{z}}_t | \mathbf{h}_t, \mathbf{x}_t)$ , and (3) transition predictor  $\tilde{\mathbf{z}}_t \sim p(\tilde{\mathbf{z}}_t | \mathbf{h}_t)$ , where  $\mathbf{x}$  represents observation,  $\mathbf{h}$  represents the deterministic latent representation, and  $\hat{\mathbf{z}}$  and  $\tilde{\mathbf{z}}$  represents the posterior and prior stochastic latent states.

PlaNet aims to learn the RSSM to generate accurate observations and rewards from a prior latent distribution for MPC planning. The dynamic model is trained by maximising the variational lower bound between prior and posterior latent states and the maximum likelihood of reconstruction of the observation and reward, where it includes an observation predictor  $\hat{\mathbf{x}}_t \sim p(\mathbf{x} | \mathbf{h}_t, \mathbf{z}_t)$  and a reward predictor  $\hat{r}_t \sim p(r | \mathbf{h}_t, \mathbf{z}_t)$ :

$$\begin{aligned} \mathcal{L}_{PlaNet} = & \sum_{t=1}^T \left( - \mathbb{E}_{q(\mathbf{z}_t | \mathbf{x}_{1:t}, \mathbf{a}_{1:t})} \left[ \log p(\mathbf{x}_t | \mathbf{z}_t) \right] \right. \\ & \left. + \mathbb{E}_{q(\mathbf{z}_{t-1} | \mathbf{x}_{1:t-1}, \mathbf{a}_{1:t-1})} \left[ KL[q(\mathbf{z}_t | \mathbf{x}_{1:t}, \mathbf{a}_{1:t}) || p(\mathbf{z}_t | \mathbf{z}_{t-1}, \mathbf{a}_{t-1})] \right] \right) \end{aligned} \quad (1)$$

Model predictive control (MPC) is a set of advanced control methods that usually require a learned/known dynamic model to predict future behaviour of the controlled system and a cost function to optimise the sampled trajectories. MPC with Cross-Entropy Method (MPC-CEM) is a common variation that samples actions from a multivariate Gaussian distribution and iteratively optimises the distribution’s mean and variance from the elite trajectories determined by the cost function. PlaNet employs MPC-CEM to produce the policy at run time by unrolling and maximising the accumulative future rewards from the latent prior distributions. It iteratively refines its latent dynamic model by exploring the environment and collecting new trajectories generated by the planner.

#### 3.2 PlaNet-Pick

Our PlaNet-Pick method is built upon the original PlaNet. We train the latent dynamic model for cloth-flattening offline using corner-biased strategy [35, 17] and scripted demonstration so that we bypass the exploration of the original algorithm. We also adopt *KL balancing* [14] to enhance posterior and prior learning, and *latent overshooting* [13] to improve multi-step prior prediction quality and robustness of the latent dynamic model. In addition, we utilise the data augmentation technique rotation [24] and flipping to improve the learning efficiency and robustness of the latent dynamic model. Furthermore, we improve the performance of the planner by clipping sampled actions between its boundary that has been used to train latent dynamics

*KL balancing:* In Equation 1, the KL-divergence term aims to learn the prior from the posterior representation and regularises the posterior representation with the prior. To avoid regularising the posterior representation

towards poor priors, Dreamer V2 [14] proposes *KL balancing* that prioritises learning of the prior over regularising the posterior. Combining the two components with an interpolation factor  $\alpha = 0.8$ , *KL balancing* achieves the former by stopping the gradient on the posterior representation and the latter by stopping the gradient on the prior representation. *KL balancing* is a significant factor for improving the asymptotic performance and learning efficiency of Dreamer [14, 15]. Section 4.3 and Section 4.6 show its significance in the cloth domain for both posterior and prior learning.

*Latent Overshooting* The latent dynamic model only learns the one-step prior distribution by default. Hafner et al. (2019) [13] also propose *latent overshooting* technique that learns a multi-step latent prior distribution, which is essential for robust long-horizon planning. Like one-step prior learning, *latent overshooting* learns the multi-step prior distribution using KL divergence between the corresponding posteriors and the priors. *Latent overshooting* also learns to predict the rewards on the multi-step priors against their ground truth value. Note that default *latent overshooting* stops the gradient of the corresponding posteriors. Even though *latent overshooting* produces more accurate multi-step priors, it does not surpass the performance of basic PlaNet on the `dm_control` benchmark [13]. In our application, we set the overshooting distance as 2 and the loss scalar for KL divergence and reward prediction from multi-step priors as 0.1 and 1. Section 4.4 and 4.6 shows its importance for robust planning, but it also comprises the planning performance with shorter planning horizons.

*Policy Generation* : In MPC-CEM, we clip the sampled actions with their boundaries  $[-0.5, 0.5]$  before feeding into the latent dynamic model to predict priors. This leads to a significant improvement in the planning quality. Since the latent dynamic model still has difficulty learning the sharp and complex transition at the contour of the cloth, we readjust the planned pick position to the closest cloth pixel if the distance is within the 5% margin on the pixel space, and we stop the operation when the cloth reaches a 95% flattened state.

## 4 Experiments

We assess manipulation performance through normalised coverage and normalised improvement across the action steps, as is standard in the cloth-flattening literature. We additionally evaluate the latent dynamic model through a combination of secondary metrics: (1) the observation reconstruction and reward prediction from posteriors give a good indication of posterior representation learning, which is important for providing good initial latent states for the MPC planning; (2) The accuracy of the prior reward prediction is an important metric for assessing the quality of the latent dynamic model, as the quality of MPC planning depends of the accurate calculation of its cost function; (3) the KL divergence between posteriors and priors, as well as the reconstruction from the priors, can assess the quality of prior learning; and (4) we want both posteriors and priors to have moderately low entropy because high-entropy states can lead the planning algorithm to generate inaccurate actions. In addition to studying the five modifications (Section 4.6), we also show the comparison of different types of latent dynamic models and their comparability to VSF (Section 4.2).

### 4.1 Dataset

We generate 1,000 random instances of cloth in the SoftGym<sup>1</sup> [27] environment to cover a wide range of shapes and positions. We reserve 100 episodes for assessing the manipulation system; the rest are for development. Following VSF [17], we manually select a subset of testing states and classify them into 5 tiers based on initial coverage (see Table 1).

Table 1: Difficulty tiers regarding Normalised Coverage (NC) of initial states.

Tier	NC Range	NC mean	NC min	NC max	No. Eps
0	$\geq 90\%$	97.12%	93.77%	99.15%	5
1	$78.3 \pm 6.9\%$	78.19%	73.26%	83%	4
2	$57.6 \pm 6.1\%$	56.12%	52.75%	60.77%	9
3	$41.1 \pm 3.4\%$	40.50%	38.1%	43.03%	10
4	$< 30\%$	28.72%	27.08%	29.94 %	5

We also generate 20,100 episodes of 50-step trajectory data from the developing settings for training the latent dynamic models. We delegate 100 episodes for testing the latent dynamic model and 20,000 episodes (1 million

<sup>1</sup>SoftGym Github: <https://github.com/Xingyu-Lin/softgym>

transitional steps) for training the models.

## 4.2 General Study on Various Latent Dynamic Models

In this experiment, we examine four different latent dynamic models: including PlaNet<sup>2</sup>, Dreamer<sup>3</sup>, Dreamer-Categorical and SLAC<sup>4</sup>.

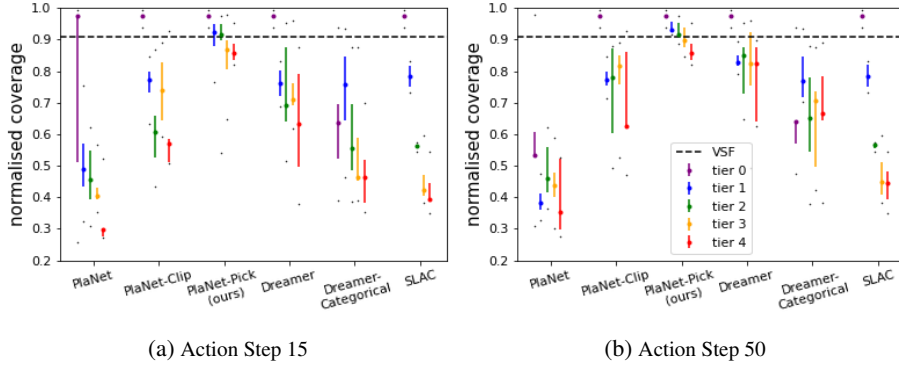


Figure 2: Planning Performance on Various Latent Dynamic Models. The result of VSF is directly adopted from Hoque et al. (2022) [17], which is the average of the Tiers 1-3. We initialise the variance of Gaussian distributions as 0.5 to examine the original PlaNet. Apart from PlaNet and VSF, all other results are produced with action clipping using MPC (10 iterations, 1000 candidates, 10% elites of candidates, and planning horizons 2). Our method PlaNet-Pick achieves SOTA performance using Latent MPC planning and we note the vast improvement over the original PlaNet.

We find that the fundamental reason PlaNet fails at cloth flattening is that the planning algorithm feeds unseen out-of-bounds actions to the dynamic model. Hence, we propose to clip the sampled actions to an upper and lower boundary before feeding into the latent dynamic model in planning. We call this model PlaNet-Clip. Figure 2 shows that clipping substantially improves planning. We also evaluate the planning performance of other dynamic models with this clipped version of MPC.

Figure 3 shows that Dreamer and SLAC produce a sharper posterior reconstruction of the observation compared to PlaNet but less accurate prior observation reconstructions. Figure 2 shows that RSSM-based models give the best results in our application, so we focus on improving the latent dynamic model of PlaNet.

## 4.3 KL Balancing

The main difference between the latent dynamic models of PlaNet and Dreamer is that Dreamer applies *KL balancing* in its prior learning. We study the effect of the KL balancing factor on both Dreamer and PlaNet.

Figure 4a shows that increasing the *KL balancing* factor produces better posterior reward prediction for both models, while its effect on prior prediction is not clear. This suggests that increasing the *KL balancing* factor increases the focus on posterior regularisation. In contrast, Figure 4b shows a reverse effect on prior prediction, with an explosion beyond factor 0.8. This suggests that increasing the *KL balancing* leads to more meaningful but more difficult prior distribution learning.

The effect of *KL balancing* is not obvious with a planning horizon 1 (see Figure 5), but leads to a great improvement in asymptotic performance and operational efficiency with planning horizon 2. This suggests that *KL balancing* leads to better prior prediction quality.

## 4.4 Latent Overshooting

A direct way to improve planning performance is to make more accurate longer-horizon predictions. This requires integrating *latent overshooting* [13] into the dynamic training. Figure 6b shows that *latent overshooting* generally

<sup>2</sup>PlaNet Github: <https://github.com/Kaixhin/PlaNet>

<sup>3</sup>Dreamer Github: <https://github.com/jsikyoon/dreamer-torch>

<sup>4</sup>SLAC Github: <https://github.com/alexlee-gk/slac>

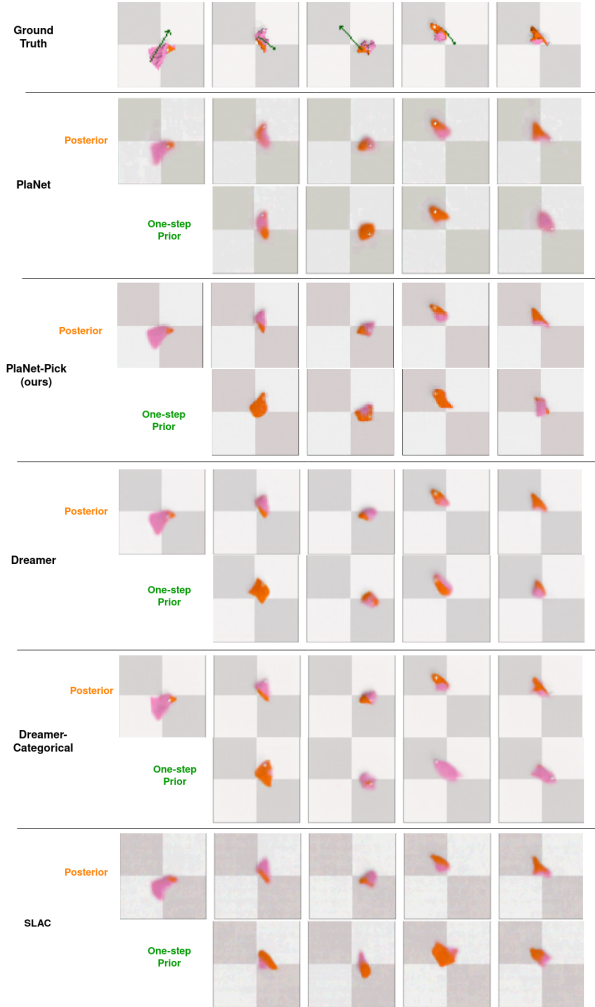


Figure 3: Observation reconstruction quality of different latent dynamic models. This is a test trajectory in the dataset, not a manipulation trajectory from planning. Models trained with *KL balancing* (PlaNet-Pick, Dreamer and Dreamer-Categorical) produce a sharper and more accurate posterior reconstruction.

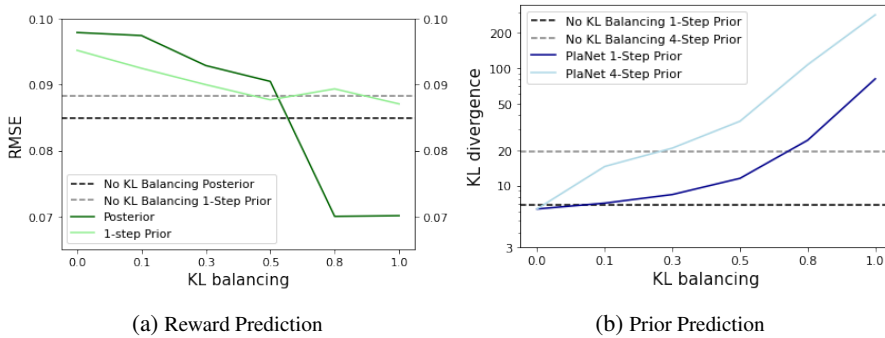


Figure 4: Effect of KL balancing on the latent dynamic model. Increasing the KL balancing factor leads to better posterior and prior reward prediction, but the prior prediction error explodes past 0.8.

produces a more robust latent dynamic model even when trained with overshooting distance 2. However, Figure 6a shows that *latent overshooting* compromises the planning performance with shorter planning horizons.

Also, longer overshooting distances generally compromise the planning performance, possibly due to spending too many resources on prior learning instead of learning posteriors. More research on this is needed on how to

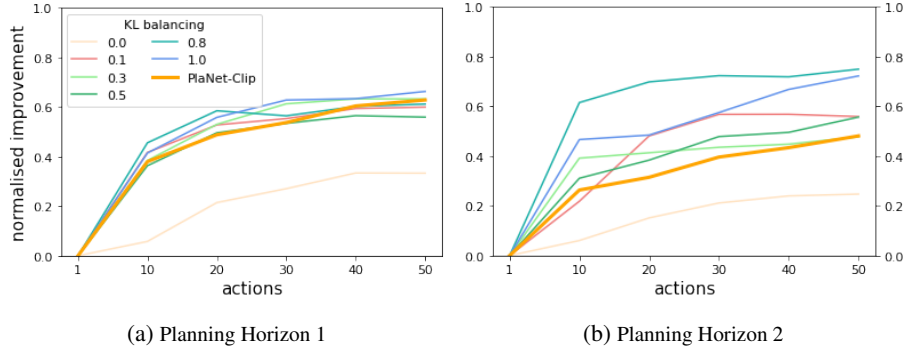


Figure 5: Effect of KL Balancing on MPC Planning (10 iterations, 1000 candidates). We skip Tier 0 and 1 evaluation here, as they start with a nearly flattened cloth. KL Balancing factor 0.8 leads to best performance.

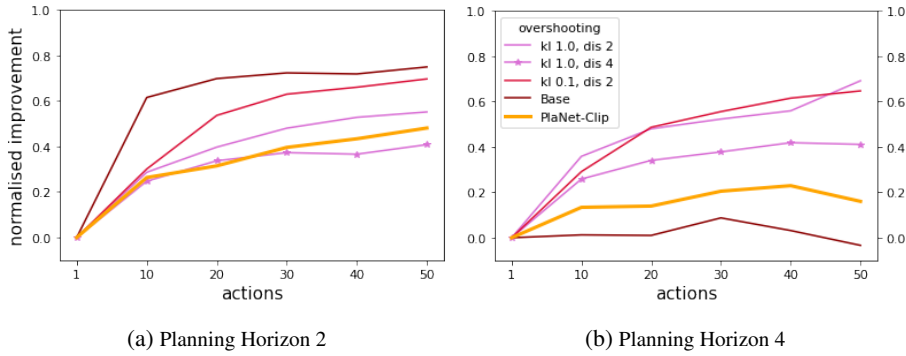


Figure 6: Effect of latent overshooting on MPC planning (10 iterations, 1000 candidates). The reward overshooting factor is 1.0. Base model is trained with KL balancing 0.8. dis represents the overshooting distance. Latent overshooting leads to more robust planning with longer planning horizons.

learn better multi-step prior while maintaining the quality of the posterior.

## 4.5 Data Augmentation

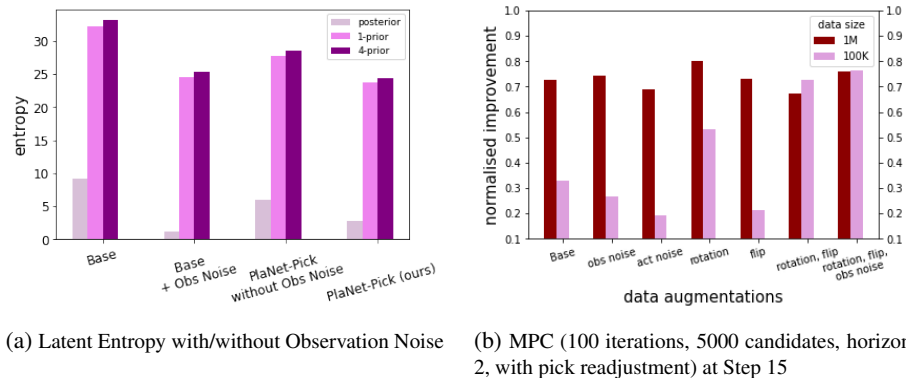


Figure 7: Effect of various Data Augmentations. Base model is trained with both *KL balancing* and *Latent overshooting*. Combination of rotation, flipping and observation noise produces the best result for models trained with smaller data size.

We apply rotation (multiples of 90 degrees), vertical flipping for data augmentation. We also apply observation noise, as in the original PlaNet implementation. Our experiments show that rotation and flipping make learning more data-efficient as they upsample the existing data. However, this augmentation does not necessarily improve

operational efficiency. Data augmentation, in general, leads to lower entropy in the latent state while keeping other metrics at the same value, but observational noise reduces the entropy more than other augmentation techniques (see Figure 7a). We also examined the effect of action noise (up to 0.25% deviation from the ground truth) but found that it harms manipulation performance for this application.

## 4.6 Ablation Study on PlaNet-Pick

We finalise our model with five modifications to the original PlaNet algorithm. We adopt *KL balancing* to improve the quality of latent state representation, *overshooting* to improve the robustness of the model for longer horizon planning and *data augmentation* to improve the data efficiency of the training. In this experiment, each of the modifications is added incrementally.

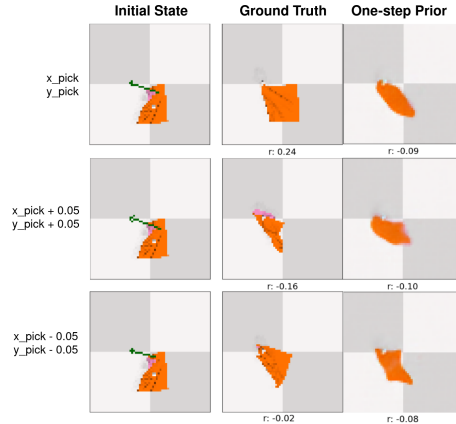


Figure 8: The effect of action precision on prediction quality of PlaNet-Pick. Latent dynamic models suffer from sharp discontinuity of the cloth’s dynamic.

We observe that the planning algorithm often produces an action slightly outside of the cloth, which always misses the cloth and makes the algorithm operationally inefficient. Corners and edges are critical for manipulating a cloth efficiently, but, as shown in Figure 8, the quality of prediction of action around the contour of the article is not sufficient. The improvement of such readjustment on the operational efficiency can be seen in Figures 9e and 9f. Apart from using the clipping trick on the action to avoid feeding unseen actions to the latent dynamic model for planning, we also apply pick readjustment as described in Section 3.2 to improve the system’s operational efficiency.

As shown in Figure 9e, the clipping trick fundamentally fixes PlaNet’s failure on the cloth-flattening domain while *KL balancing* drastically improves its manipulation performance. Based on Figures 9a and 9b, *KL balancing* allows focusing on posterior representation learning that intuitively provides a better starting latent posterior state for planning. *Latent overshooting*, on the other hand, reduces the difference between posterior and multi-step prior distribution (see Figure 9c) that, in turn, makes the latent dynamic more robust while planning with longer horizons (see Figure 9f).

## 5 Conclusion

This paper thoroughly explores the application of latent dynamic models on cloth flattening. We apply action clipping, *KL balancing*, *latent overshooting*, data augmentation, and pick readjustment to improve its performance and robustness in cloth flattening. Our method PlaNet-Pick achieve state-of-the-art performance using latent MPC, more than doubling the performance of the original PlaNet algorithm. To our knowledge, this is the first time an RSSM-based model has shown state-of-the-art performance on the cloth flattening task.

### 5.1 Discussion

We find that the precision of the pick position directly influences the performance of the latent dynamic planning — the model cannot accurately predict the transition of the cloth if the pick position is close to the contour of



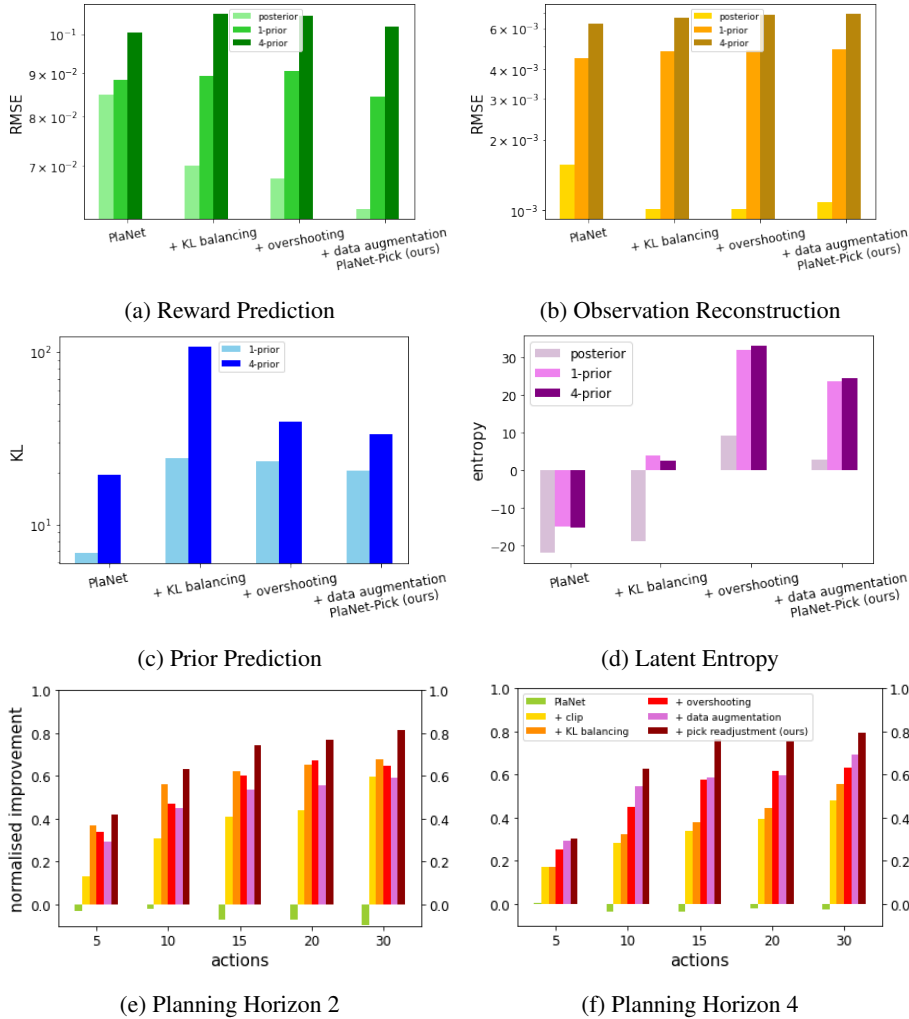


Figure 9: Effect of Modifications. MPC (100 iterations, 5000 candidates). *KL balancing* improves posterior learning, *latent overshooting* improves robustness, and *pick readjustment* improves operational efficiency.

the cloth. Applications of RSSM-based methods in other pick-and-place domains, such as peg-and-hole [41] and cube-stacking tasks [22], may also fail where high precision of both pick and place actions is required. In addition, there are still potential improvements in *latent overshooting* for more robust planning.

*Why are we insisting on latent dynamic learning?* A famous quote related to Alfred North Whitehead says, "The purpose of thinking is, so our thoughts die instead of us." Planning is an important part of human decision-making; we especially do it for complex and long-horizon tasks. We can do it because we can imagine and simulate scenarios and causality in our brains. Humans have another decision-making process built into our motor skills, which is more similar to policy learning rather than planning. Despite not explicitly simulating events after mastering a skill, we still need an inference-generative process to refine the automatic subconscious prediction of our sensory information, known as predictive processing [31, 8] in cognitive science literature. It resembles the idea of world model [9] and latent dynamic model [13] with variational inference in modern robotics.

## 5.2 Future

There are several directions of future work we want to explore. First, we want to investigate further the action precision and multi-step prior learning issues in latent dynamic learning. We also want to investigate the exploration competence of PlaNet that we avoided in this paper. Second, using variational latent dynamic models in robotics and the RL community based on RSSM and control as an inference framework shows significant improvements in planning and policy learning. While this paper focuses on planning with latent dynamic models, we also want to

examine the policy learning counterpart of these models in the future — certainly, exploration will be an obstacle for this investigation. We also want to investigate SOTA adversarial inverse reinforcement learning algorithms in this domain.

Third, we want to investigate the applications of planning and policy learning methods based on a latent dynamic model in more complex cloth-shaping tasks [20, 35]. Finally, another important aspect of animal motor control is hierarchical predictive processing. Hierarchical sequential VAE [3] presents a vast improvement in video prediction compared to its simple one-layer model counterpart [6], but for stable training, it requires layers-by-layers training [36].

## References

- [1] Jimmy Lei Ba, Jamie Ryan Kiros, and Geoffrey E Hinton. Layer normalization. *arXiv preprint arXiv:1607.06450*, 2016.
- [2] Marc G Bellemare, Yavar Naddaf, Joel Veness, and Michael Bowling. The arcade learning environment: An evaluation platform for general agents. *Journal of Artificial Intelligence Research*, 47:253–279, 2013.
- [3] Lluís Castrejon, Nicolas Ballas, and Aaron Courville. Improved conditional vrnns for video prediction. In *Proceedings of the IEEE/CVF International Conference on Computer Vision*, pages 7608–7617, Seoul, Korea, 27 October–2 November 2019.
- [4] Junyoung Chung, Çağlar Gülçehre, KyungHyun Cho, and Yoshua Bengio. Empirical evaluation of gated recurrent neural networks on sequence modeling. *CoRR*, abs/1412.3555, 2014.
- [5] Djork-Arné Clevert, Thomas Unterthiner, and Sepp Hochreiter. Fast and accurate deep network learning by exponential linear units (elus). *arXiv preprint arXiv:1511.07289*, 2015.
- [6] Emily Denton and Rob Fergus. Stochastic video generation with a learned prior. In *International conference on machine learning*, pages 1174–1183. PMLR, 2018.
- [7] Frederik Ebert, Chelsea Finn, Sudeep Dasari, Annie Xie, Alex X. Lee, and Sergey Levine. Visual foresight: Model-based deep reinforcement learning for vision-based robotic control. *CoRR*, abs/1812.00568, 2018.
- [8] Karl Friston, Thomas FitzGerald, Francesco Rigoli, Philipp Schwartenbeck, and Giovanni Pezzulo. Active inference: a process theory. *Neural computation*, 29(1):1–49, 2017.
- [9] David Ha and Jürgen Schmidhuber. World models. *arXiv preprint arXiv:1803.10122*, 2018.
- [10] Huy Ha and Shuran Song. Flingbot: The unreasonable effectiveness of dynamic manipulation for cloth unfolding. In *Conference on Robot Learning*, pages 24–33, Auckland, New Zealand, 15–18 Decemeber 2022. PMLR.
- [11] Tuomas Haarnoja, Aurick Zhou, Pieter Abbeel, and Sergey Levine. Soft actor-critic: Off-policy maximum entropy deep reinforcement learning with a stochastic actor. In *International conference on machine learning*, pages 1861–1870, Stockholm, Sweden, 10–15 July 2018. PMLR.
- [12] Danijar Hafner, Timothy Lillicrap, Jimmy Ba, and Mohammad Norouzi. Dream to control: Learning behaviors by latent imagination. In *International Conference on Learning Representations*, Addis Ababa, Ethiopia, 26–30 April 2020.
- [13] Danijar Hafner, Timothy Lillicrap, Ian Fischer, Ruben Villegas, David Ha, Honglak Lee, and James Davidson. Learning latent dynamics for planning from pixels. In *International Conference on Machine Learning*, pages 2555–2565, Long Beach, CA, USA, 10–15 June 2019. PMLR.
- [14] Danijar Hafner, Timothy P Lillicrap, Mohammad Norouzi, and Jimmy Ba. Mastering atari with discrete world models. In *International Conference on Learning Representations*, 2021.
- [15] Danijar Hafner, Jurgis Pasukonis, Jimmy Ba, and Timothy Lillicrap. Mastering diverse domains through world models. *arXiv preprint arXiv:2301.04104*, 2023.

- [16] Ryan Hoque, Daniel Seita, Ashwin Balakrishna, Aditya Ganapathi, Ajay Kumar Tanwani, Nawid Jamali, Katsu Yamane, Soshi Iba, and Ken Goldberg. Visuospatial foresight for multi-step, multi-task fabric manipulation. *CoRR*, abs/2003.09044, 2020.
- [17] Ryan Hoque, Daniel Seita, Ashwin Balakrishna, Aditya Ganapathi, Ajay Kumar Tanwani, Nawid Jamali, Katsu Yamane, Soshi Iba, and Ken Goldberg. Visuospatial foresight for physical sequential fabric manipulation. *Autonomous Robots*, 46(1):175–199, 2022a.
- [18] Ryan Hoque, Kaushik Shivakumar, Shrey Aeron, Gabriel Deza, Aditya Ganapathi, Adrian Wong, Johnny Lee, Andy Zeng, Vincent Vanhoucke, and Ken Goldberg. Learning to fold real garments with one arm: A case study in cloud-based robotics research. *CoRR*, abs/2204.10297, 2022b.
- [19] Zixuan Huang, Xingyu Lin, and David Held. Mesh-based dynamics with occlusion reasoning for cloth manipulation. *arXiv preprint arXiv:2206.02881*, 2022.
- [20] Halid Abdulrahim Kadi and Kasim Terzić. Data-driven robotic manipulation of cloth-like deformable objects: The present, challenges and future prospects. *Sensors*, 23(5):2389, 2023.
- [21] Leslie Pack Kaelbling, Michael L Littman, and Anthony R Cassandra. Planning and acting in partially observable stochastic domains. *Artificial intelligence*, 101(1-2):99–134, 1998.
- [22] Alex X Lee, Coline Manon Devin, Yuxiang Zhou, Thomas Lampe, Konstantinos Bousmalis, Jost Tobias Springenberg, Arunkumar Byravan, Abbas Abdolmaleki, Nimrod Gileadi, David Khosid, et al. Beyond pick-and-place: Tackling robotic stacking of diverse shapes. In *5th Annual Conference on Robot Learning*, Auckland, New Zealand, 14–18 December 2021.
- [23] Alex X Lee, Richard Zhang, Frederik Ebert, Pieter Abbeel, Chelsea Finn, and Sergey Levine. Stochastic adversarial video prediction. *arXiv preprint arXiv:1804.01523*, 2018.
- [24] Robert Lee, Daniel Ward, Vibhavari Dasagi, Akansel Cosgun, Juxi Leitner, and Peter Corke. Learning arbitrary-goal fabric folding with one hour of real robot experience. In *Conference on Robot Learning*, pages 2317–2327, London, UK, 11 November 2021. PMLR.
- [25] Sergey Levine. Reinforcement learning and control as probabilistic inference: Tutorial and review. *arXiv preprint arXiv:1805.00909*, 2018.
- [26] Xingyu Lin, Yufei Wang, Zixuan Huang, and David Held. Learning visible connectivity dynamics for cloth smoothing. In *Conference on Robot Learning*, pages 256–266, Auckland, New Zealand, 5–18 December 2022. PMLR.
- [27] Xingyu Lin, Yufei Wang, Jake Olkin, and David Held. Softgym: Benchmarking deep reinforcement learning for deformable object manipulation. In *Conference on Robot Learning*, pages 432–448, London, UK, 8–11 November 2021. PMLR.
- [28] Xiao Ma, David Hsu, and Wee Sun Lee. Learning latent graph dynamics for deformable object manipulation. *CoRR*, abs/2104.12149, 2021.
- [29] Thomas M Moerland, Joost Broekens, and Catholijn M Jonker. A framework for reinforcement learning and planning. *arXiv preprint arXiv:2006.15009*, 2020.
- [30] Tobias Pfaff, Meire Fortunato, Alvaro Sanchez-Gonzalez, and Peter Battaglia. Learning mesh-based simulation with graph networks. In *International Conference on Learning Representations*, 2021.
- [31] Michał Piekarski et al. Understanding predictive processing. a review. *AVANT. Pismo Awangardy Filozoficzno-Naukowej*, (1):1–48, 2021.
- [32] Daniel Seita, Pete Florence, Jonathan Tompson, Erwin Coumans, Vikas Sindhwani, Ken Goldberg, and Andy Zeng. Learning to rearrange deformable cables, fabrics, and bags with goal-conditioned transporter networks. In *2021 IEEE International Conference on Robotics and Automation (ICRA)*, pages 4568–4575, Xi’an, China, 30 May–5 June 2021. IEEE.

- [33] Daniel Seita, Nawid Jamali, Michael Laskey, Ajay Kumar Tanwani, Ron Berenstein, Prakash Baskaran, Soshi Iba, John Canny, and Ken Goldberg. Deep transfer learning of pick points on fabric for robot bed-making. In *The International Symposium of Robotics Research*, pages 275–290, Hanoi, Vietnam, 6–10 October 2019. Springer.
- [34] Yuval Tassa, Yotam Doron, Alistair Muldal, Tom Erez, Yazhe Li, Diego de Las Casas, David Budden, Abbas Abdolmaleki, Josh Merel, Andrew Lefrancq, et al. Deepmind control suite. *arXiv preprint arXiv:1801.00690*, 2018.
- [35] Thomas Weng, Sujay Man Bajracharya, Yufei Wang, Khush Agrawal, and David Held. Fabricflownet: Bimanual cloth manipulation with a flow-based policy. In *Conference on Robot Learning*, pages 192–202, Auckland, New Zealand, 15–18 December 2022. PMLR.
- [36] Bohan Wu, Suraj Nair, Roberto Martin-Martin, Li Fei-Fei, and Chelsea Finn. Greedy hierarchical variational autoencoders for large-scale video prediction. In *Proceedings of the IEEE/CVF Conference on Computer Vision and Pattern Recognition*, pages 2318–2328, Stockholm Sweden, 10–15 July 2021.
- [37] Yilin Wu, Wilson Yan, Thanard Kurutach, Lerrel Pinto, and Pieter Abbeel. Learning to manipulate deformable objects without demonstrations. *arXiv preprint arXiv:1910.13439*, 2019.
- [38] Zhenjia Xu, Cheng Chi, Benjamin Burchfiel, Eric Cousineau, Siyuan Feng, and Shuran Song. Dexterity: Deformable manipulation can be a breeze. In *Proceedings of Robotics: Science and Systems (RSS)*, New York, NY, USA, 27 June–1 July 2022.
- [39] Wilson Yan, Ashwin Vangipuram, Pieter Abbeel, and Lerrel Pinto. Learning predictive representations for deformable objects using contrastive estimation. In *Conference on Robot Learning*, pages 564–574, London, UK, 8–11 November 2021. PMLR.
- [40] Yuxiang Yang, Ken Caluwaerts, Atil Iscen, Tingnan Zhang, Jie Tan, and Vikas Sindhwani. Data efficient reinforcement learning for legged robots. In *Conference on Robot Learning*, pages 1–10, Cambridge, MA, USA, 14–16 November 2020. PMLR.
- [41] Harry Zhang, Jeffrey Ichnowski, Daniel Seita, Jonathan Wang, Huang Huang, and Ken Goldberg. Robots of the lost arc: Self-supervised learning to dynamically manipulate fixed-endpoint cables. In *2021 IEEE International Conference on Robotics and Automation (ICRA)*, pages 4560–4567, Xi’an, China, 30 May–5 June 2021. IEEE.
- [42] Brian D Ziebart, Andrew L Maas, J Andrew Bagnell, Anind K Dey, et al. Maximum entropy inverse reinforcement learning. In *Aaai*, volume 8, pages 1433–1438. Chicago, IL, USA, 2008.

# APPENDIX

## 5.3 Environment Configuration

Most of our environment settings are inherited directly from SoftGym’s `ClothFlattenEnv`. As the original environment does not support pixel-based pick-and-place actions, we add corresponding functionality by a picking height of 0.02 m and a placing height of 0.15m above the surface — the picker particle with a radius of 0.02m first reaches the target position in pixel-space and lowers its height to the set value, then it picks up a cloth particle if the distance between the cloth particle and the picker is within 0.002m; consequently, the picker raises to the placing height and drag the cloth to the target placing position then drop the cloth.

In addition, we fix the target article as a  $0.4m \times 0.4m$  square fabric with orange and pink colours at its different surfaces. With a particle radius of 0.00625m and allowing overlapping for simulating the cloth-like behaviour, the cloth comprises  $64 \times 64$  particles. Following SoftGym’s default setting, the cloth-like properties, such as stretch, bend and shear, of the target object are set as (0.8, 1, 0.9) individually. Lastly, we set the height of the top-down camera as 1.5m above the surface. Note that the pixel-to-world ratio is 0.415 when the distance toward the camera centre is 1.

## 5.4 Initial State Generation

We generated 1,000 random instances of cloth in the SoftGym environment and selected the first 100 for evaluating manipulations and the rest for development. We use the initial state generation strategy described below to cover a wide range of shapes and positions.

For each instance, a perfectly flattened cloth is initially placed at the centre of the world, with the orange side facing up and edges parallel to the horizontal dimension of the world. Then, the picker uniformly picks a particle on the cloth, lifts the particle by a random height from 0 to 0.4m, and drops it on the floor. Consequently, the oracle centres the cloth randomly within the  $0.3 \times 0.3$  square-meter boundaries. Finally, 70% of the time, the picker again randomly chooses a cloth particle and drags it by a random vector to the height of 0.1m, where the horizontal values of the vector are within  $[-0.3m, 0.3m]$  range; lastly, it drops the particle from this position and recentres it within the  $0.3 \times 0.3$  square-meter boundaries.

## 5.5 Trajectory Data Collection

To accelerate the development, we trained the models offline, requiring the dataset to cover various state-action dynamics. We incorporated a scripted demonstration policy to include the trajectories that can lead to successful flattening in the dataset. As picking on edge and corner is the effective action for this task, we also include trajectories produced by a scripted corner-biased policy [35, 17]. Since the state-action dynamic is highly complex and sensitive, especially to the picking action, we add noises on the demonstration and corner-biased picking policy to cover the sharp transitional variance at the contour of the cloth. Each episode is sampled with an alternative 10-step noisy demonstration and a 10-step corner-biased policy.

**Demonstration Policy** We scripted a demonstration policy that can access the oracle of the environment. It focuses on operating on the corners of the cloth, as it is the most effective way to flatten it. At each step, the policy determines a target flattening position for the corners by sweeping through  $[-0.3m, 0.3m]$  along x-y coordinates with an interval of 0.01m. Then, it selects to operate on the corner closest to its target position. If the corner is visible, the place action drags it directly to the target position. Otherwise, the policy drags the visible particle right above the chosen corner in the opposite direction by the same distance towards the target position to reveal the corner and reserve the target dragging position for the next step.

**Corner-biased Policy** Corner-biased policy, on the other hand, selects the pick position from the output of the Harris corner detector on the grey-scaled observation, which operates 45% of the time in this policy. Another, 45% of the time, the pick position is sampled from the oracle’s true corners of the cloth. The rest of the 10% of the time is chosen uniformly within the boundaries of the action space. In contrast, the placing position is always chosen uniformly within the boundaries of the action space.

## 5.6 Details of PlaNet’s Implementation

**Model Architecture** There are three main components of an RSSM model: the recurrent dynamic model, the representation model, and the transition predictor. Diagonal normal distributions represent the stochastic latent states  $\mathbf{z}$ . The reparameterisation trick produces the sampling of the stochastic latent states. The final standard deviation is firstly calculated by applying `softplus` on the output standard deviation and adding a minimum value of 0.1. The initial deterministic and stochastic latent states ( $\mathbf{h}_0, \mathbf{z}_0$ ) are set to  $\mathbf{0}$  before the starting of each trajectory. In the default setting, the deterministic state is set to 200, and the stochastic ones are set to 30.

In default PlaNet, the recurrent dynamic model is implemented with GRU cell [4] to produce a deterministic latent state for each time step  $\mathbf{h}_t$  — it takes  $\mathbf{h}_t$ , and embeddings of  $(\mathbf{z}_t, \mathbf{a}_t)$  as inputs and produces  $\mathbf{h}_{t+1}$ . The transition predictor is implemented as a linear layer that produces the stochastic prior latent state  $\tilde{\mathbf{z}}_{t+1}$  by taking embedding of  $\mathbf{h}_{t+1}$  as input. When the embedding of the observation  $\mathbf{e}_{t+1}$  is given, the representation model, also a linear layer, produces the stochastic posterior  $\hat{\mathbf{z}}_{t+1}$  is from the embedding of  $(\mathbf{h}_{t+1}, \mathbf{e}_{t+1})$ . Note that all the embedding layers are one linear layer that outputs the embedding dimension as 200 with `relu` activation.

The observation  $\mathbf{e}$  embeddings are produced by a vision encoder comprising four convolutional layers with `relu` activation in between. The kernel and stride sizes of these convolutional layers are 4 and 2. The output channels are (32, 64, 128, and 256). The encoder takes RGB images  $\mathbf{x}_t$  with size  $3*64*64$  as input to output embedded codes  $\mathbf{e}_t$  with size 1024.

For posterior learning, PlaNet utilises a vision decoder to reconstruct RGB observations  $\hat{\mathbf{x}}_t$  from the latent states  $(\mathbf{h}_t, \mathbf{z}_t)$ . It comprises of 4 layers transposed convolutional layers with kernel sizes (5, 5, 6, 6) and strides of 2. The output channels are (128, 64, 32, and 3). A reward predictor is required for MPC planning, which comprises three linear layers with hidden dimensions of 200 and `relu` activation in between. It takes both latent states  $(\mathbf{h}_t, \mathbf{z}_t)$  as input and predicts the corresponding reward  $\hat{r}_t$ .

**Training Details** We train the models in an end-to-end fashion with 100,000 update steps — this applies to all latent dynamic training in this paper. At each update step, the latent dynamic model takes a batch of 50 trajectories (allowing to cross consecutive episodes) with a sequence length of 50 from the replay buffer and produces reconstructed rewards and observations from the sampled posteriors. Note that if an episode ends in a sampled trajectory, we need to reset the states  $\mathbf{0}$ s while unrolling with the transition model. PlaNet adds small Gaussian noises on observation at bit depth 5 and maps the pixels from [0, 255] to [-0.5, 0.5] before feeding them into the model. The vision decoder also produces pixel values between [-0.5, 0.5].

The loss function comprises of an observation MSE loss between the ground truth  $\mathbf{x}$  and the reconstruction  $\hat{\mathbf{x}}$  (mean over the steps after summing over the pixels), a reward MSE loss (purely mean), and KL divergence from the stochastic posteriors  $\hat{\mathbf{z}}$  to the stochastic priors  $\tilde{\mathbf{z}}$ . The KL loss for each transitional step is computed by getting the maximum between the free-nat of 3 and the sum over the latent dimension. All 3 component losses have scalar 1.0 in the final loss function. An adam optimiser is employed with a learning rate of  $1e-3$  and eps  $1e-4$ , and the norms of the backpropagated gradients are clipped to 1000 before each parameter updates.

## 5.7 Dreamer’s Latent Dynamic Model

The training and architecture of Dreamer V2’s latent dynamic model are similar to the one of PlaNet but with several differences. As in architecture, Dreamer V2 employs `elu` [5] for activation between the layers and GRU with layer normalisation [1] as the transition predictor. Dreamer has a stochastic layer of 50.

As for training, Dreamer V2 does not add small Gaussian noises on observation and does not allow sampling across episode trajectories. PlaNet has deterministic outputs for reward and observation reconstruction. It uses MSE for the prediction loss, while Dreamer outputs stochastically and uses negative log-likelihood (NLL) for posterior learning and reward prediction. Fourth, the final standard deviation  $std'$  of stochastic latent code is calculated from the inference network  $std$  output using  $std' \leftarrow 2 * \text{sigmoid}(std/2) + 0.1$ . Moreover, PlaNet learns the prior distribution and regularises the posterior distribution simultaneously with a single KL divergence term and free bits 3. At the same time, Dreamer adopts *KL balancing* factor of 0.8 to separate and balance the two processes with free bit 1. Lastly, it uses an adam optimiser with a learning rate  $3e-4$  and eps  $1e-5$ , and the norms of the backpropagated gradients are clipped to 100 before each parameter updates.

**Categorical** The Categorical version of the Dreamer has its stochastic latent states as categorical distribution instead of Gaussian distribution. This version of the Dreamer shows substantial improvement on Atari games but does not perform as well as its Gaussian counterpart in `dm_control` continuous control domain [14]. To

avoid hyper-parameter tuning, we directly inherit the default setting of the categorical version of the Dreamer that is used to solve Atari games, where the stochastic latent dimension is 32, and each dimension is a 32-labelled categorical distribution. The stochastic latent state  $\mathbf{z}$  is flattened before putting into other component layers of the model. Reward layers have four dimensions, and convolutional depths as 48 instead of 32. The KL scale is set to 0.1 instead of 1.0. Other settings are the same as the ones in Gaussian Dreamer.

## 5.8 SLAC’s Latent Dynamic Model

SLAC [23] does not have a recurrent cell in the latent dynamic model as in RMSS-based models, but it has two layers of stochastic latent space  $(\mathbf{z}^1, \mathbf{z}^2)$ . All the stochastic networks are two layers with a hidden dimension of 64, and the standard deviation is activated with `softplus` function with  $1e-5$  as an addition. The models’ weights are initialised with `xavier_uniform` with gain 1.0, while the bias term is initialised to 0. It uses `leaky_relu(0.2)` for all activations. In training, it leverages the NLL loss function.

The initial first layer stochastic latent code  $\mathbf{z}_1^1$  is set to standard diagonal normal distribution. The prior of the first layer stochastic latent states for other times step  $\tilde{\mathbf{z}}_{t+1}^1$  is produced from the  $(\mathbf{z}_t^2, \mathbf{a}_t)$ . The posterior  $\hat{\mathbf{z}}_{t+1}^1$  is produced from  $(\mathbf{e}_{t+1}, \mathbf{z}_t^2, \mathbf{a}_t)$ . The initial second layer stochastic latent code  $\mathbf{z}_1^2$  is inferred from the initial first latent code  $\mathbf{z}_1^1$ . All other second layer stochastic latent codes  $\mathbf{z}_{t+1}^2$  are produced from  $(\mathbf{z}_{t+1}^1, \mathbf{z}_t^2, \mathbf{a}_t)$ . The vision decoder takes  $(\mathbf{z}_t^1, \mathbf{z}_t^2)$  to predict the distribution of  $\hat{\mathbf{x}}_t$ , and the reward predictor takes  $(\mathbf{z}_t^1, \mathbf{z}_t^2, \mathbf{a}_t, \mathbf{z}_{t+1}^1, \mathbf{z}_{t+1}^2)$  as input to predict  $\hat{r}_t$ .

The vision encoder composes of 5 convolutional layers with output dims as (32, 64, 128, 256, and 256), kernel size as (5, 3, 3, 3, and 4), strides as (2, 2, 2, 2, and 1), and paddings as (2, 1, 1, 1, and 0). The vision decoder composes of 5 transposed convolutional layers with output dims as (256, 128, 64, 32, and 3), kernel sizes as (4, 3, 3, 3, and 5), strides as (1, 2, 2, 2, and 2), paddings as (0, 1, 1, 1, and 2), and output paddings as (0, 1, 1, 1, and 1).

## 5.9 Failure Cases

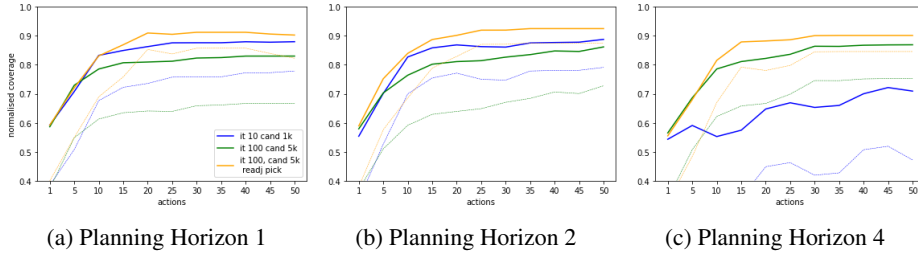


Figure 10: MPC Performance of PlaNet-Pick. The thin dashed lines represent the value of one standard deviation below the mean. The evaluation is based on all tiers.

As shown in Figure 10, PlaNet-Pick with pick-position readjustment is agnostic to different planning horizons. Nevertheless, insufficient searching comprises the method’s performance when the planning horizon is longer than its training overshooting distance.

As shown in the first action of PlaNet-Pick in Figure 1, some misgrasping actions are still happening. Also, the final coverage is stuck around 90%; because the latent dynamic model thinks the cloth is already flattened and predicted close to a reward as 1, no further actions are needed. In addition, rigid P&P (where the placing height and the lower-level trajectory are fixed) cannot flatten the article perfectly by nature.